Till genesis and glacier motion inferred from sedimentological evidence associated with the surge-type glacier, Brúarjökull, Iceland

Anna E. NELSON,[1*] Ian C. WILLIS,[1] Colm Ó COFAIGH[2]

[1]*Scott Polar Research Institute, University of Cambridge, Lensfield Road, Cambridge CB2 1ER, UK*
E-mail: aene@bas.ac.uk
[2]*Department of Geography, University of Durham, South Road, Durham DH1 3LE, UK*

ABSTRACT. A study employing macro- and micro-sedimentological techniques was conducted at three sites with recently deglaciated sediments in the proglacial area of Brúarjökull, a surge-type outlet glacier of the Vatnajökull ice cap, Iceland. Tills at these sites were likely deposited and deformed during the 1963/64 surge. At the height of the last surge, these sediments were beneath 90–120 m of ice, and associated basal shear stresses would have been 24–32 kPa. Tills associated with the surge at these sites formed by a combination of subglacial sediment deformation and lodgement and are thus regarded as 'hybrid tills'. The tills show evidence of both ductile and brittle deformation. Discontinuous clay lenses within the tills, indicating local ice–bed decoupling and sliding, imply that subglacial water pressures were spatially and temporally variable during the surge. The thickness of the subglacial deforming-till layer was 50–90 cm.

INTRODUCTION

Movement at the base of temperate ice masses resting on soft sediment is accomplished by basal sliding and/or subglacial sediment deformation. Establishing the hydrological and mechanical controls on ice–bed coupling, the partitioning between sliding and sediment deformation and how this partitioning varies in space and time are important areas of glaciological research (e.g. Boulton and others, 2001; Fischer and Clarke, 2001). They are important for improved understanding of: (i) short-term variations in glacier velocity (Iverson and others, 1994; Fischer and others, 1999; Mair and others, 2003); (ii) glacier surging (Clarke, 1987; Raymond, 1987); (iii) ice-stream flow and the stability of the West Antarctic ice sheet (Alley and others, 1989; Engelhardt and Kamb, 1998); and (iv) the advance and retreat of Quaternary ice sheets (Piotrowski and Tulaczyk, 1999; Ó Cofaigh and Evans, 2001). Conceptual models based on a combination of theoretical analyses and field evidence suggest that subglacial drainage, subglacial water-pressure regime and till properties combine to determine the relative contribution of sliding and sediment deformation (Boulton and Hindmarsh, 1987; Alley, 1989; Boulton and others, 2001; Fischer and Clarke, 2001). At low water pressures, ice is well coupled to the bed and basal motion may occur through enhanced ice deformation and regelation around bedrock bumps and limited brittle shear within sediments (Boulton and Hindmarsh, 1987; Benn, 1994b; Benn and Evans, 1996). At moderate water pressures, sediment strength is reduced, encouraging ductile deformation, and ice–bed coupling is reduced, encouraging limited sliding (Boulton and Hindmarsh, 1987; Alley, 1989; Hart and Boulton, 1991). At high water pressures, ice–bed decoupling is extensive, producing uplift and rapid sliding (Iverson and others, 1995, 2003). This decreases the effective normal stress on sediments, allowing them to squeeze into the zone of uplift and thicken (Iverson and others, 1995) or to undergo elastic relaxation (Fischer and Clarke, 2001; Iverson and others, 2003). The decrease in effective normal stress will also weaken the sediments, encouraging ploughing of clasts through the sediment surface (Iverson and others, 1995, 2003; Fischer and Clarke, 2001).

As subglacial processes often leave a sedimentary signature (cf. Hart and Rose, 2001), we adopt a sedimentological approach to the study of subglacial processes beneath a surge-type glacier in Iceland. We use a combination of macro- and micro-sedimentological techniques in an attempt to infer the extent of ice–bed coupling, the balance of sliding vs sediment deformation, and the styles (brittle vs ductile) and pervasiveness (depth) of sediment deformation beneath the glacier.

FIELD SITE DESCRIPTION

Brúarjökull is a northern outlet glacier of the Vatnajökull ice cap, southeast Iceland (Fig. 1). This surge-type glacier covers an area of ~1700 km^2, is ~45 km long from the ice-cap summit to the glacier snout, ranges in elevation from 550 to 1900 m a.s.l. and has an average surface slope of ~1.7° (Sigurðsson, 1998; Björnsson and others, 2003).

The surges of Brúarjökull are the most dramatic in Iceland, with advances of ~8–10 km during the active phase, and a surge period of 70–100 years (Thórarinsson, 1969; Sigurðsson, 1998). Known surges occurred in 1963, 1890, 1810 and possibly 1625 (Thórarinsson, 1964). During the most recent surge of 1963/64, the glacier advanced ~8 km at maximum rates of ~100 m d^{-1}. It affected ~1400 km^2 of land and may have been triggered by high accumulation rates in 1960–61 (Thórarinsson, 1964). The glacier has since retreated ~3–4 km (Knudsen and Marren, 2002).

Five major rivers drain Brúarjökull: Kreppa, Kverká, Sauðá, Kringilsá and Jökulsa á Dal (Fig. 1). This study is

*Present address: British Antarctic Survey, Natural Environment Research Council, Madingley Road, Cambridge CB3 0ET, UK.

https://doi.org/10.3189/172756405781812961 Published online by Cambridge University Press

located in the glacier forefield between the Kverká and Sauðá rivers (Fig. 1). The forefield is dominated by shallow flutes, up to ~100 m long and up to ~1 m thick (Fig. 2a), which are thought to have been formed during a single glacier advance (Evans, 2003). Concertina eskers in the forefield are up to ~40 m long and ~7 m thick and are thought to relate to the most recent 1963/64 surge (Knudsen, 1995; Evans, 2003). Crevasse-squeezed diamict ridges are also evident in the proglacial area and can be traced back to the crevasses of the present-day ice surface (Fig. 2a). These were likely produced during the waning stages of the last surge, when water-saturated basal sediments were squeezed up into surge-induced basal crevasses (Evans and others, 1999; Evans, 2003). Similar ridges were first described in front of the neighbouring surge-type glacier Eyjabakkajökull (Sharp, 1985).

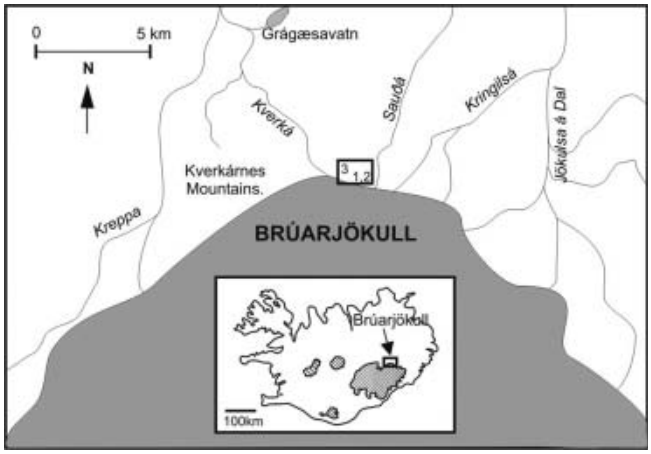

Fig. 1. Brúarjökull field site location. Large black rectangle represents locations of sites 1–3. Map of Iceland (inset) indicates location of Brúarjökull.

METHODOLOGY

Three natural exposures, the only natural exposures observed in the entire forefield of Brúarjökull between the Kverká and Sauðá rivers, were examined. Vertical sections at each exposure were logged and information on sediment texture, lithology, sedimentary structures and bedding contacts was recorded and facies subsequently identified (cf. Eyles and others, 1983). The sections were photographed, and scaled section drawings made (Figs 2 and 3).

Quantitative sedimentological measurements of clast roundness, shape and fabric strength were obtained from diamict facies, similar to the procedures employed by Fuller and Murray (2002). Samples of 30 clasts were chosen at random for these measurements.

The roundness of the 30 clasts was measured using the scale of Powers (1953). Clasts were put into one of five classes (very angular, angular, subangular, subrounded or rounded). Additionally, the 'RA' summary index, i.e. the percentage of angular and very angular clasts within a sample, was calculated (Benn and Ballantyne, 1993). Roundness refers to the degree of curvature of clast edges and is a useful indicator of erosional history when used in combination with clast shape (Benn and Ballantyne, 1994). Boulton (1978) defined an active mode of transport, in the basal traction zone, and a passive mode of transport, above the traction zone. Subangular- to angular-shaped clasts (with high RA indices) would tend to suggest supraglacially derived and passively transported material, whereas subrounded- to rounded-shaped clasts (with low RA indices) would imply active transport in the traction zone (Boulton, 1978).

The lengths of the three clast axes were also measured and their relationships were plotted on equilateral ternary diagrams and used to define clast shape (Benn, 1994a). They were also used to calculate the C_{40} index, i.e. the percentage of clasts with a $c:a$ axis ratio <0.4 (Benn and Ballantyne, 1993, 1994). A low C_{40} index would mean that the clasts have compact, blocky shapes. As the clasts consist of coarse-grained lithologies, this may imply that they had fractured across their long axis and undergone active transport at high stresses (Benn and Ballantyne, 1994). Conversely, a high C_{40} index would mean the clasts have more elongate and slabby shapes, suggesting they may have undergone more high-level transport with minimal comminution at low stresses (Benn and Ballantyne, 1994).

The orientation and dip of the 30 clasts were also measured with a compass clinometer and used to determine

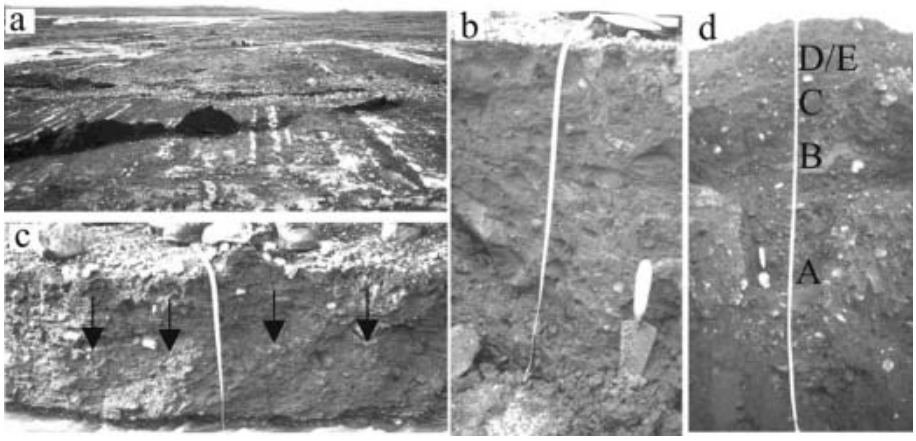

Fig. 2. (a) Photograph of the forefield of Brúarjökull, taken from the ice margin, showing flutes and crevasse-filled ridges. People in background are at site 1. (b) Site 1 (80 cm): massive, matrix-supported fissile diamict. (c) Site 2 (50 cm): massive, matrix-supported fissile diamict with attenuated clay lenses (arrowed). (d) Site 3 (220 cm): cobble-rich fluvial sediment (units A–C) overlain by two-tiered diamict (units D and E).

https://doi.org/10.3189/172756405781812961 Published online by Cambridge University Press

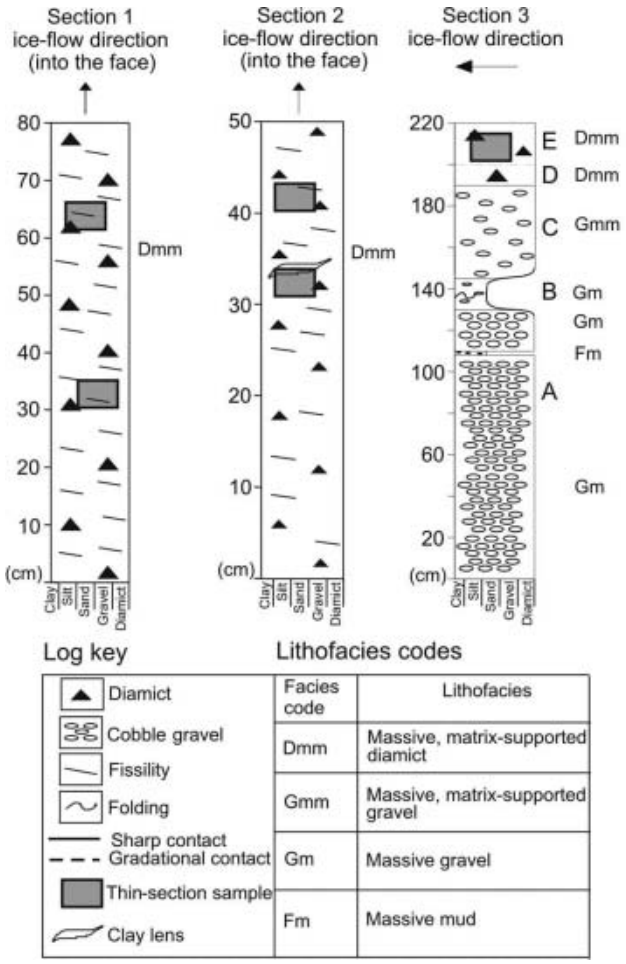

Fig. 3. Lithofacies logs of sites 1–3. The shaded boxes represent locations of micromorphology samples.

fabric strength. The *a*-axis fabric data were plotted on stereographic plots to determine if the clasts had a preferred orientation and/or dip. The eigenvalues of each unit (S_1–S_3) are values representing the magnitude of clustering around the respective orthogonal eigenvectors (V_1–V_3) and can be helpful when inferring depositional processes and strain history in tills (Dowdeswell and Sharp, 1986; Benn 1994a, 1995; Hart 1994).

For each diamict facies, 1 kg bulk samples of the <2 mm size fraction were collected. The matrix particle-size distribution of each sample was determined subsequently using a combination of dry-sieving for the >1 mm size fraction and a laser particle-size analyser (Malvern Mastersizer X©) for the <1 mm size fraction. Grain-size distribution is also an indicator of transport path and degree of deformation (Boulton, 1978; Hooke and Iverson, 1995).

Blocks of sediment were collected from selected diamict units for subsequent micromorphological analysis. For each sample, ~30 cm of surface sediment was initially removed from the face. A Kubiëna tin was then pressed into the face and carefully removed using a penknife. The sediment samples were wrapped in cling film to prevent moisture loss during transport to the laboratory. In the laboratory, the samples were air-dried, impregnated with resin, and cut and mounted on glass slides (Van der Meer, 1987; Fuller and Murray, 2000). A thin section, oriented parallel to the face of the exposure, was prepared from each sample and viewed under a microscope at magnifications of 4 and 10 using both plain and cross-polarized light. The thin sections were described using terminology originally developed for soils but adapted specifically for glacial sediments (Van der Meer 1987, 1993). In the descriptions, the grains are the particles that are discerned individually, whereas the plasma or matrix is the material that is too fine to observe as individual grains, usually <20 μm (Van der Meer, 1987). The aim of the micromorphological analysis was to investigate the presence and type of deformation structures within the sediments, and to use these, together with the macro-sedimentological data, to infer the style of sediment deformation.

In the following section, we use all of these methods and lines of evidence in combination to describe and interpret the sediments in terms of their most likely transport and depositional history.

SEDIMENTOLOGY

Site 1 description

This site is located ~50 m from the present-day ice front. The ground surface is prominently fluted with flutes up to ~100 m long and ~50 cm thick, which record a former ice-flow direction toward 30° northeast. An outwash stream flowing obliquely to the flutes at 340° northwest has cut into the sediment exposure. The 25 m long section is in the down-glacier stream bank, and faces towards the glacier at 250° southwest (Fig. 2b).

The section consists of an 80 cm thick, dark-brown, stiff, matrix-supported diamict (Fig. 3). The well-consolidated, highly fissile diamict has a muddy matrix with 10–15% clasts and appears structurally and texturally uniform throughout its thickness. 65% of the clasts are pebbles, and 35% gravels. Striations or other signs of clast–clast interaction were not observed on the clast surfaces.

Macro-sedimentological data were collected from the upper and lower parts of the section (Fig. 4; Table 1). The particle size distribution, clast angularity, clast shape and fabric data are very similar at the two locations. In both cases, the particle size distribution is bimodal, with peaks in the coarse-silt/fine-sand (4/5ϕ) and gravel (–1ϕ) fractions. The high percentage of subangular and subrounded clasts results in low RA indices <10. The clast-shape ternary diagrams show a diamict dominated by blocky clasts, with C_{40} indices <10. There is a strong fabric (S_1 = 0.754 and 0.678) dipping in the down-glacier direction. The main sedimentological differences between the upper and lower parts of the section are that the upper part has less coarse material and fewer very blocky clasts than the lower part.

Micromorphological samples were taken from the upper and lower parts of the section (Fig. 2). The only microstructure observed in the lower part is grain fracture, where a single basalt grain is fractured into two pieces (Fig. 5a). Microstructures observed in the upper part include circular structures and sub-horizontal lineaments (Fig. 5b and c). The circular structures are composed of coarse silt-sized tephra and basalt clasts oriented around a basalt core stone. The sub-horizontal lineaments are present throughout the sample and dip at ~0–10° to the west.

Site 2 description

This site is located ~7 m up-glacier from site 1. It has exactly the same geomorphic setting as site 1. Thus, the section is in

https://doi.org/10.3189/172756405781812961 Published online by Cambridge University Press

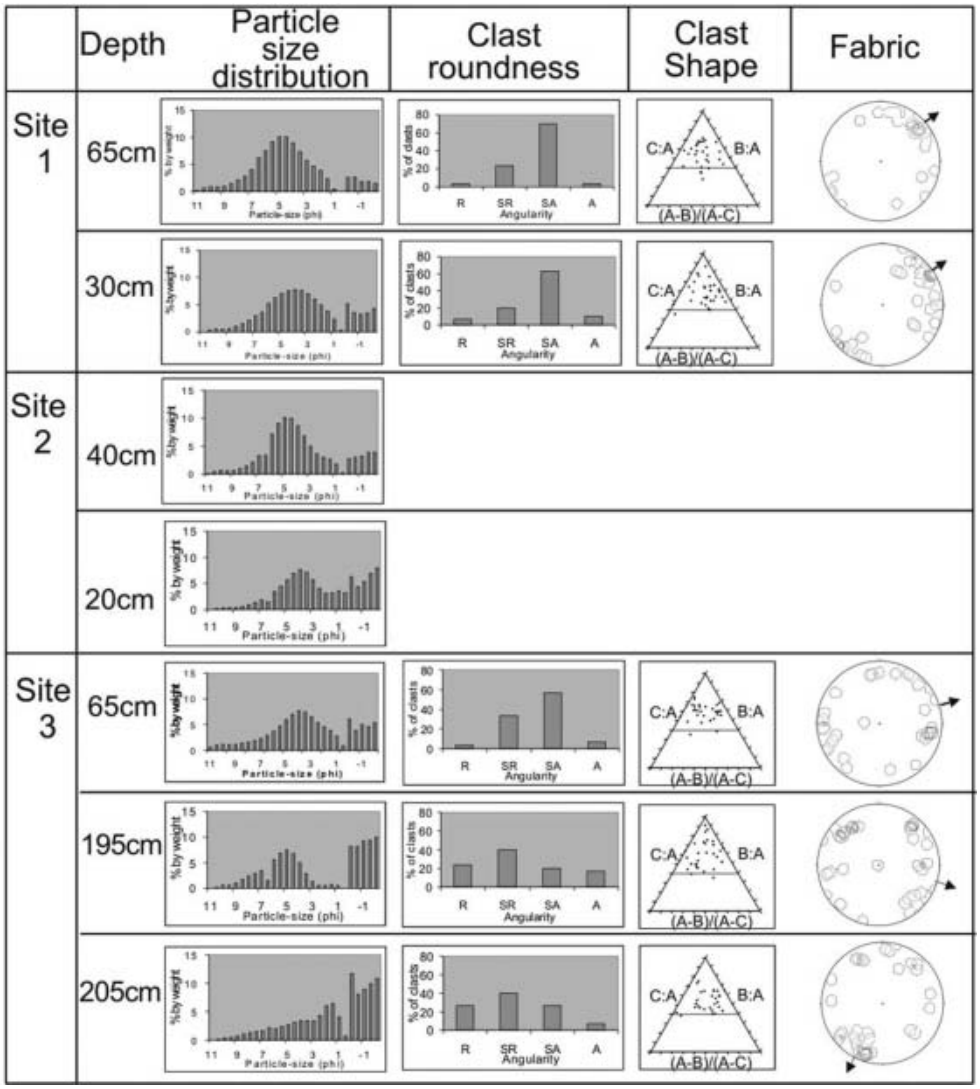

Fig. 4. Sediment characteristics of units within sites 1–3 of Figure 3. The troughs between 1ϕ and 0ϕ may be artifacts of sieving.

the down-glacier bank of a stream, which faces towards the glacier at 250° southwest (Fig. 2c).

The section consists of a 50 cm thick, dark-brown, well-consolidated, matrix-supported, fissile diamict (Fig. 3). As at site 1, the diamict has a muddy matrix and contains 10–15% clasts (65% pebbles, 35% gravels). Striae were not observed on the clasts. Discontinuous intermittent clay lenses occur within the diamict along the length of the 25 m long exposure. The lenses are 5–7 cm wide, 1–1.5 cm thick and dip towards the eastern end of the exposure, orthogonal to present-day ice-flow direction.

Detailed clast data could not be obtained from this site, as the undercutting stream limited accessibility. However, bulk sediment samples were collected for particle size from both the upper and lower parts of the exposure, and micromorphological samples were collected from the upper and lower/middle parts of the exposure. As at site 1, the particle size distributions from the lower and upper parts of the

Table 1. Sediment characteristics of each unit described in the sediment logs of Figure 3. PSD: particle size distribution; S_1–S_3 are eigenvalues

	Depth	PSD peaks	RA index	C_{40} index	S_1	S_2	S_3
Site 1	65 cm	5, –0.5	7	10	0.754	0.195	0.051
	30 cm	4, –1	10	7	0.678	0.233	0.089
Site 2	40 cm	5, –1.5					
	20 cm	4, –2					
Site 3	Unit E 65 cm		7	7	0.592	0.286	0.122
	Unit D 195 cm	5, –1	17	7	0.518	0.329	0.154
	Unit C 205 cm	–2	7	3	0.615	0.242	0.143

https://doi.org/10.3189/172756405781812961 Published online by Cambridge University Press

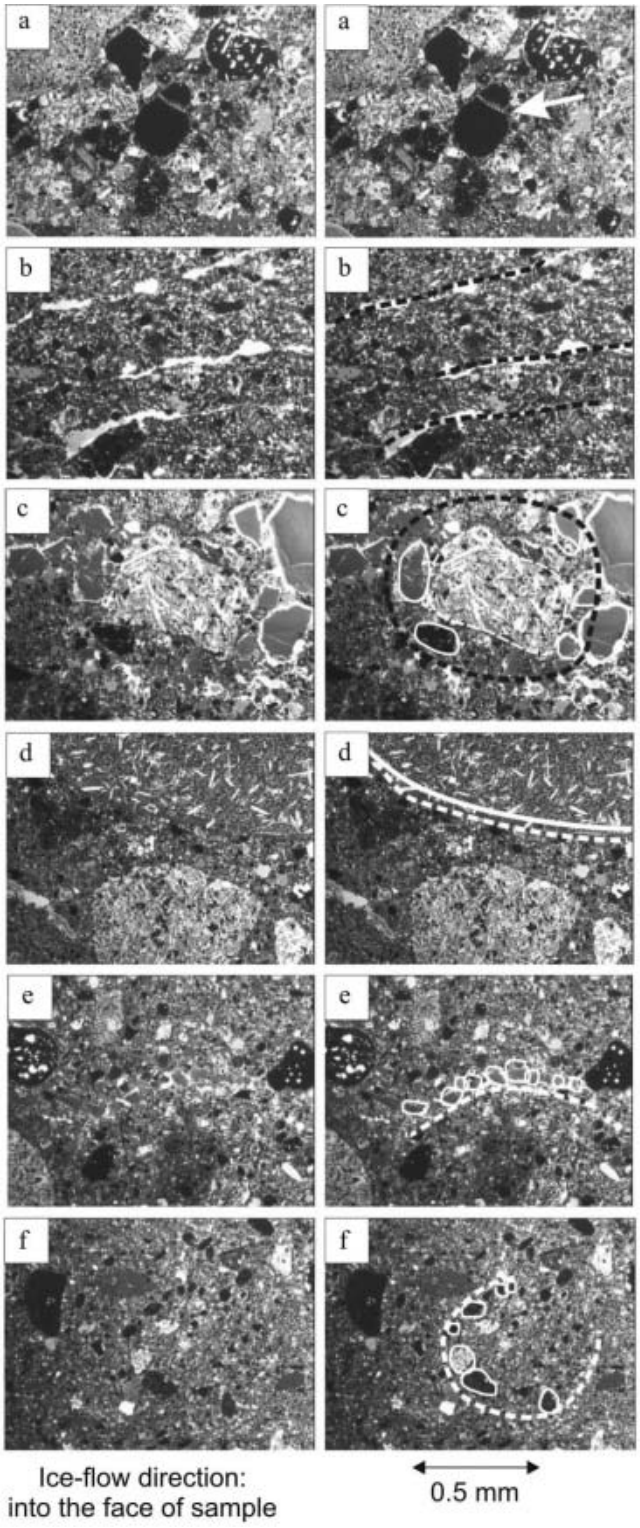

Fig. 5. Photomicrographs of sites 1 and 2. Slides on the left are originals. Slides on the right have been annotated to highlight important features referred to in the text. (a) Grain fracture (arrowed) from lower part of site 1. (b) Fissility from upper part of site 1. (c) Circular structure with basalt core stone from middle part of site 2. (d) Silt drape beneath basalt clast from middle part of site 2. (e) Sub-horizontal lineament from middle part of site 2. (f) Circular structure without core stone from upper part of site 2.

exposure are similar (Fig. 4). The dominant peak in both samples is centred on the coarse-sand/fine-silt (4–5ϕ) fraction. The upper sample has a small secondary peak centred on the gravel (–1.5ϕ) fraction, whereas the lower sample contains a higher percentage of material between 2ϕ and –2ϕ with no obvious peak.

The thin section obtained from the lower/middle part of the exposure sampled the clay lenses described above. In thin section, the lenses are fractured and attenuated. The lenses show circular structures with core stones (Fig. 5c), while the bounding diamict shows clay coatings, clay drapes (Fig. 5d), sub-horizontal lineaments (Fig. 5e), necking structures, pressure shadows, folds, and circular structures without core stones (Van der Meer, 1993). There are clay boudins, as well as clay coatings and drapes, on the underside and top of coarse clasts (Fig. 5d). Pressure shadows and folds also occur in the zone around the lenses. There is a necking structure composed of three coarse basalt clasts in close proximity to one another. A line of fine basalt and tephra clasts emerges from between two of these clasts.

There are few microstructures in the upper part of the section, and they are limited to only occasional circular structures and fissility (Fig. 5f). The circular structures are defined by the alignment of clasts around an intraclast rather than a core stone.

Sites 1 and 2 interpretation

The diamicts at sites 1 and 2 are interpreted as subglacial tills, based on the following criteria:

1. The presence of flutes which overlie the sites and indicate that they have been glacially overridden.
2. The massive, fissile nature of the diamicts. Such fissility is commonly regarded as a product of subglacial shear (Boulton and others, 1974; Hart and Boulton, 1991; Benn, 1994b).
3. The bimodal or multi-modal particle-size distributions, and, at site 1, the low RA index, and blocky clasts, which indicate active transport in the zone of basal traction where abrasion and crushing occur (Boulton, 1978).
4. The fabric orientation of the diamict at site 1 is consistent with the direction of ice flow recorded by the flutes, and the high S_1 values suggest subglacial transport and ice–bed coupling (Benn, 1995; Evans, 2000).
5. The micromorphological data show the diamicts contain a range of structures which indicate that they have been deformed at the microscale, including lineaments, circular structures, necking structures, pressure shadows and folds. Lineaments are typical of discrete shear zones within clay-rich material and support the interpretation of the fissility as the product of subglacial shear. Circular structures with core stones are interpreted as the product of grain rotation in a till matrix undergoing ductile deformation (Van der Meer, 1997; Van der Meer and others, 2003). The evidence for both brittle (shear planes: fissility and lineaments) and ductile (circular structures) deformation operating within the till unit implies that the deformation was polyphase (Van der Meer, 1993; Menzies, 2000).

Subglacial tills can form by a variety of end-member processes including melt-out, lodgement and deformation, or some combination of each. These processes can vary spatially and temporally across a glacier bed, with tills formed by one process subsequently being modified by another (e.g. an initial phase of lodgement followed by subglacial deformation (Benn and Evans, 1998)). The

https://doi.org/10.3189/172756405781812961 Published online by Cambridge University Press

resulting tills contain a variety of diagnostic characteristics at both a macro- and microscale, but rarely can their genetic interpretation be based or just one or two criteria.

The diamicts at sites 1 and 2 are unlikely to be subglacial melt-out tills, for four reasons. First, although thick, debris-rich, basal ice sequences have been observed at the temperate Matanuska Glacier, Alaska, USA, (Lawson, 1979) they are generally associated with non-temperate glaciers (e.g. Souchez and others, 1988; Knight, 1994) and we have not observed them around the current margin of Brúarjökull. Second, even if such thick debris-rich, basal ice sequences did exist at Brúarjökull, it is unlikely that they would have produced unmodified subglacial melt-out tills since the poor drainage conditions around the present glacier margin suggest that reworking is exceptionally common where ice is melting (cf. Paul and Eyles, 1990; Benn and Evans, 1998). Third, although deformation structures may be preserved in debris-rich basal ice and sometimes preserved in the resulting till following basal melt-out, we consider it unlikely that, in cases where drainage conditions are poor such as at Brúarjökull, the delicate microscale deformation structures that we observe in thin sections from sites 1 and 2 would be retained in unmodified form in the resulting till. Fourth, the presence of flutes which overlie the site implies that even if some unmodified subglacial melt-out till had been deposited, it was subsequently overridden by the glacier and would likely have been subjected to subglacial deformation and/or lodgement. Thus, although it is possible that melt-out as a *process* locally occurred beneath the glacier sole, we do not consider the diamicts at sites 1 and 2 to be melt-out tills.

Lodgement tills are formed where sediment is plastered from the glacier sole onto the bed by either pressure melting or direct lodging of clasts (generally large cobble to boulder in size). During the lodgement process, debris is subjected to crushing and abrasion. The resulting till is characteristically massive, overconsolidated and fissile, with bimodal or multimodal grain-size distributions and strong fabrics. Typically clasts have rounded edges, striated and faceted surfaces, and larger clasts in particular may have a bullet-shaped appearance with stoss and lee faces (Boulton, 1978). Several of the characteristics that we record in the diamicts at sites 1 and 2 are consistent with deposition by lodgement: fissility, grain-size, the stiff matrix and strong fabrics. Such features, however, have also been documented in deformation tills (Boulton and Dent, 1974; Boulton and others, 1974; Benn, 1995). The S_1 values that we record are consistent with field-based studies of deformation till (Benn, 1995; Evans, 2000) but are lower than those based on experimental studies (Hooyer and Iverson, 2000). The micromorphological data show that the tills contain a range of structures indicative of brittle and ductile subglacial deformation (see above), in the form of circular structures, lineaments (shear planes), folds and necking structures (Van der Meer and others, 2003). Striations were not observed on clast surfaces within the diamicts and neither were bullet-shaped boulders, both of which might be expected where tills are formed by lodgement. The presence of the intact but deformed units of clay in site 2 is also important to note. Such fine-grained sediments would have a low preservation potential, where lodgement is the dominant mechanism of till formation, and would likely be homogenized into the surrounding till matrix by the lodgement process. We therefore believe that *collectively* the above characteristics are consistent with an origin for the tills at sites 1 and 2 by a combination of subglacial deformation and lodgement. The diamicts at both sites are thus a type of hybrid till in which the two end-member processes of sediment deformation and lodgement operated together.

The clay lenses contained within the till at site 2 are inferred to be deposits from a thin water film that formed as the ice temporarily separated from the bed (cf. Van der Meer, 1987; Piotrowski and Tulaczyk, 1999; Fuller and Murray, 2000, 2002). The clay lenses occur across the full 25 m lateral extent of the section and within a vertical zone of 20 cm. Their lateral continuity argues against the lenses being deformed rafts of clay within the till (Fuller and Murray, 2000). The fact that the clay units are fractured and attenuated implies that the ice subsequently recoupled to the bed and deformed the lenses by brittle and ductile shear.

Site 3 description

This site is located ~70 m from the present-day ice margin (Fig. 2d). The overlying flutes are ~50 m long, ~80 cm thick and they record a former ice-flow direction toward 30° northeast. The section is located in the down-glacier bank of a stream, and faces toward the glacier at 350° northwest. An adjacent esker is ~40 m long and ~7 m high. The exposure is 220 cm high and consists of five units (Fig. 3).

Unit A

The lowermost 130 cm of the section consists of clast-dominated, massive boulder gravel with 60% cobbles and boulders. Clasts are mainly rounded and lack striations. Within this unit is a 2 cm thick, massive, poorly consolidated, muddy gravel at 110 cm depth.

Unit B

Above the lowermost boulder gravel is 15 cm of tectonized cobble gravel with 40% clasts. Macroscale deformation structures in the form of attenuated clay lenses and folded pockets of silt, sand and gravel occur in the unit.

Unit C

Overlying the tectonized cobble gravel is 45 cm of clast-supported cobble gravel. This gravel is similar to unit B, but contains fewer boulders and more sand. It also contains pockets of iron staining. Its particle size distribution (Fig. 4) shows a steady increase in concentration toward the larger fraction, peaking at –2ϕ. The clasts are mainly subrounded or rounded, giving a low RA index of 7, while their blocky shapes produce a very low C_{40} index of 3. There is a moderate fabric ($S_1 = 0.615$) dipping in the up-glacier direction. The main feature of this unit is the high number of clasts with fractured surfaces. The fractures generally occur across their long axes, resulting in clasts with both angular and rounded edges (recorded as 'subrounded'), and giving an overall blocky shape.

Unit D

A two-tiered diamict (units D and E) overlies the non-tectonized cobble gravel. The lowermost 10 cm is a massive, well-consolidated, matrix-supported diamict with 5–10% clasts. The unit has a bimodal particle-size distribution with a peak in the fine-sand (5ϕ) fraction, although there is also a high percentage of gravel-sized particles (Fig. 4). The clasts are particularly angular, with a high RA index of 17. The predominantly blocky clasts give a low C_{40} index of 7.

https://doi.org/10.3189/172756405781812961 Published online by Cambridge University Press

There is a moderate fabric ($S_1 = 0.518$), orthogonal to ice-flow direction.

Unit E

The uppermost unit is 20 cm thick and iseparated from the underlying diamict by a gradational contact. It is a matrix-supported, massive, well-consolidated, mud-rich diamict with only 0–5% clasts. The clasts have a low RA index of 7, predominantly blocky clast shapes, a low C_{40} index of 7, and a moderately strong fabric ($S_1 = 0.592$) dipping in the east-northeast direction (Fig. 4). At 205 cm, there is an attenuated clay band ~60 cm long and ~0.5 cm thick. This is entombed within the diamict matrix and is most likely a sediment raft.

A micromorphological sample was taken at 205 cm, which included the attenuated end of the clay band as well as the surrounding diamict. The clay is massive and contains 5% grains (mostly sands and silts). It is attenuated and brecciated. The clay lens is truncated by a basalt clast that has pushed the remainder of the lens tail deep into the sediment beneath. Just beyond this tectonized tail is a clay boudin that has been detached from the lens. There are also multiple circular structures with core stones. There is an area of discrete lineaments with grain alignments in an east–west orientation. Some grains also have silt caps.

Site 3 interpretation

Units A–C are interpreted as high-energy fluvial deposits, based on the following criteria: (1) the gravel-rich, highly porous material; and (2) the silt and sand layers within units A and B which suggest fluctuations in current strength. Both units B and C were subjected to deformation, which is inferred to have occurred subsequent to their deposition, with ductile deformation affecting unit B (folding) and brittle deformation affecting unit C (fractured clasts).

Units D and E are interpreted as a type of hybrid till formed by a combination of subglacial sediment deformation and lodgement at the glacier sole. This interpretation is based on the following criteria: First, the diamicts are massive, although unlike the diamicts at the other two sites they are not fissile. Unit E, however, contains a deformed clay raft. Second, the diamicts are underlain by deformed glaciofluvial gravels. Third, micromorphological data show brittle (boudinage, shear zones), ductile (circular structures, folding) and pore-water-influenced (silt caps) deformation structures, implying polyphase deformation (Van der Meer, 1993). Fourth, the relatively strong clast fabric is oriented in the direction of ice flow, indicating significant coupling between the ice and underlying sediment (Benn, 1995; Evans, 2000). Fifth, the bimodal particle-size distribution indicates crushing and abrasion in the zone of basal traction (Boulton, 1978) and is consistent with particle size distributions associated with lodgement tills (Dreimanis, 1988; Benn and Evans, 1998). Thus, as in the case of the tills at sites 1 and 2, the diamict unit at site 3 is inferred to be a type of hybrid till in which subglacial sediment deformation during overriding of the glaciofluvial gravels acted together with lodgement to form units D and E.

DISCUSSION

Relationship of the sediment to surges of Brúarjökull

All three sites are located within 100 m of the current ice margin and would have been 3–4 km up-glacier from the margin at the end of the 1963/64 surge. Assuming a current ice surface slope of 1.7° means that the sites would have been under 90–120 m of ice, and basal shear stresses would have been 24–32 kPa at the height of the last surge. The flutes were likely formed during the last surge (Knudsen, 1995; Evans, 2003), and as there is no obvious erosional contact between the flutes and the underlying diamicts, we assume the tills are also a product of the 1963/64 surge. Furthermore, the macro-sedimentological evidence for deformation of the fluvial sediments underlying the tills at site 3 suggests they too were deformed during the last surge. There is no obvious unconformity between the tills and the fluvial deposits at site 3, suggesting the fluvial sediments immediately predate the tills and that the tills are sourced from the gravels. The fluvial sediments at site 3 were likely deposited proglacially during the 1890–1962 quiescent phase. During the subsequent surge, the glacier advanced over the gravels, deformed them and reworked them into the overlying till represented by units D and E. The sedimentary sequence at site 3 bears similarities to the gravel-outwash/deforming-till continuum described at Skálafellsjökull, Iceland, by Evans (2000).

Deformation vs sliding

The subglacial tills that we document in the forefield of Brúarjökull contain elements consistent with formation by both subglacial sediment deformation and lodgement. We thus interpret the diamicts at these sites as hybrid tills formed by a combination of subglacial sediment deformation and lodgement. Evidence for deformation of the sediments is present at the macro- and microscale in the form of high fissility, brecciated and attenuated clay lenses, rotational and planar deformation structures. This evidence indicates that Brúarjökull deformed its bed during the last surge, and implies that sediment deformation contributed to the rapid motion of the glacier during the surge event. However, our evidence varies slightly from the classic two-tier deformation till (upper ductile horizon and lower brittle/ductile horizon) described for Breiðamerkurjökull, Iceland (Boulton and Hindmarsh, 1987; Benn, 1995), in that the tills at Brúarjökull are interpreted as having formed by a combination of both subglacial sediment deformation and lodgement. In addition, the deformation structures in the upper part of site 1 and the upper till at site 3 show microscale evidence for both brittle *and* ductile deformation. Finally the capping till at site 2 is fissile and is not pervasively deformed. This implies that deformation style varied spatially and temporally during the 1963/64 surge as the tills were deposited and deformed (Hicock and Fuller, 1995; Menzies, 2000).

Temporally variable water pressures during the 1963/64 surge are suggested by the presence of discontinuous clay lenses within the till at site 2, which are observed throughout the 25 m length of the exposure. The lenses suggest local ice–bed separation and therefore sliding at high water pressures. Similar lenses were observed in tills associated with the last surge of Hagafellsjökull Vestari, Iceland, and were also attributed to ice–bed decoupling (Fuller and Murray, 2000). Ice–bed decoupling at high water pressures has been measured on other glaciers at driving stresses similar to those that would have existed at sites 2 and 3 during the last surge (Iverson and others, 1994; Fischer and Clarke, 1997). Water flow and sediment mobilization in a thin film at the ice–bed interface have also been measured at

https://doi.org/10.3189/172756405781812961 Published online by Cambridge University Press

high water pressures on other glaciers (Hubbard and others, 1995; Stone and Clarke, 1996). We envisage that the subsequent deposition of such sediment accounts for the clay lenses observed in our study. The best-documented glacier surge is the 1982/83 surge of Variegated Glacier, Alaska (Kamb and others, 1985). During the surge, subglacial water pressures were close to ice overburden; water moved slowly beneath the glacier in a distributed subglacial drainage system and was released in flood events associated with decreases in water pressure and surface velocity. We envisage that the clay lenses observed at Brúarjökull would have been deposited during such temporary decreases in water pressure. The glacier would then have recoupled to the bed and subsequently lodged and deformed the overlying till. The attenuation and brecciation of the clay lenses shows they were subsequently deformed as water pressures dropped and ice recoupled to the bed.

This variation between sliding and sediment deformation is inferred to reflect variations in subglacial effective pressure. At low effective pressure, pore-water pressures are high, and ice/bed decoupling occurs with rapid motion by basal sliding. As the effective pressure increases due to falling water pressures, the ice recouples to the bed and deforms the substrate. Our data imply that variations between sliding and subglacial sediment deformation (controlled by variations in subglacial effective pressure) occurred spatially and temporally beneath Brúarjökull.

Thickness of the subglacial deforming layer

Previous estimates of the thickness of the subglacial deforming layer from Icelandic glaciers with similar driving stresses to Brúarjökull range from ~20 cm on Hagafellsjökull Vestari (Fuller and Murray, 2000) to ~45 cm on Breiðamerkurjökull (Boulton and Hindmarsh, 1987). Deforming-layer thicknesses of ~30–65 cm have also been measured from direct observations beneath contemporary glaciers – again with similar driving stresses to Brúarjökull – in Sweden and North America (Blake, 1992; Humphrey and others, 1993; Iverson and others, 1994). Collectively these data indicate a deforming-layer thickness of <1 m. Our Brúarjökull data support this. At site 3, a maximum thickness of 90 cm for the deforming layer is provided by the depth from the top of unit E to the top of unit A (undeformed gravel). Site 1 consists of a fissile diamict that is structurally and texturally uniform throughout its thickness. This implies that the diamict at site 1, whose base is not exposed in the section, is a single till unit, and hence that the deforming layer at this site was on the order of 80 cm.

Fuller and Murray (2000) found undeformed clay lenses at depths of 16–20 cm in the forefield of Hagafellsjökull Vestari, and used these to constrain the maximum deforming-layer thickness at their sites during the most recent surge. Clay lenses are also present within the till at site 2 in the forefield of Brúarjökull. These lenses are interpreted as evidence for high pore-water pressure and transient decoupling of the glacier from its bed (see above). If the lenses are assumed to mark the base of the deforming layer, a thickness of 15–40 cm for the deforming layer is implied. However, unlike at Hagafellsjökull Vestari, the clay lenses at site 2 are themselves *deformed*. This deformation is inferred to have occurred during recoupling of the ice to its bed and emplacement of the till that caps the sequence at site 2. Preservation of the lenses indicates either that deformation was not pervasive or that the lenses were not transported far in the deforming layer and so were not homogenized. Thus the deforming layer at site 2 would have incorporated the clay lenses and could have been on the order of 50 cm (the thickness of the section). In conclusion, our data therefore indicate a deforming-layer thickness of ~50–90 cm during the most recent surge of Brúarjökull.

ACKNOWLEDGEMENTS

We thank Newnham College, the Brian Roberts Fund, the Philip Lake II Fund, the Scandinavian Studies Fund (all University of Cambridge) and the Silver Cottage Parent Fund for financially supporting this work. We also thank H. Björnsson, A. Russell and F. Tweed for logistical support in Iceland, S. Boreham and J. Miller for laboratory support, and A. Matney for fieldwork support. Comments by R. Hindmarsh, J. Hart and an anonymous referee helped us make significant improvements to the paper.

REFERENCES

Alley, R.B. 1989. Water-pressure coupling of sliding and bed deformation: II. Velocity–depth profiles. *J. Glaciol.,* **35**(119), 119–129.

Alley, R.B., D.D. Blankenship, S.T. Rooney and C.R. Bentley. 1989. Sedimentation beneath ice shelves – the view from Ice Stream B. *Marine Geology,* **85**(2/4), 101–120.

Benn, D.I. 1994a. Fabric shape and the interpretation of sedimentary fabric data. *J. Sediment. Res.,* **64A**(4), 910–915.

Benn, D.I. 1994b. Fluted moraine formation and till genesis below a temperate valley glacier: Slettmarkbreen, Jotunheimen, southern Norway. *Sedimentology,* **41**(2), 279–292.

Benn, D.I. 1995. Fabric signature of subglacial till deformation, Breiðamerkurjökull, Iceland. *Sedimentology,* **42**(5), 735–747.

Benn, D.I. and C.K. Ballantyne. 1993. The description and representation of particle shape. *Earth Surf. Process. Landforms,* **18**(7), 665–672.

Benn, D.I. and C.K. Ballantyne. 1994. Reconstructing the transport history of glacigenic sediments: a new approach based on the co-variance of clast form indices. *Sediment. Geol.,* **91**(1–4), 215–227.

Benn, D.I. and D.J.A. Evans. 1996. The interpretation and classification of subglacially-deformed materials. *Quat. Sci. Rev.,* **15**(1), 23–52.

Benn, D.I. and D.J.A. Evans. 1998. *Glaciers and glaciation.* London, Arnold.

Björnsson, H., F. Pálsson, O. Sigurðsson and G.E. Flowers. 2003. Surges of glaciers in Iceland. *Ann. Glaciol.,* **36**, 82–90.

Blake, E.W. 1992. The deforming bed beneath a surge-type glacier: measurement of mechanical and electrical properties. (PhD thesis, University of British Columbia.)

Boulton, G.S. 1978. Boulder shapes and grain-size distributions of debris as indicators of transport paths through a glacier and till genesis. *Sedimentology,* **25**(6), 773–799.

Boulton, G.S. and D.L. Dent. 1974. The nature and rates of post-depositional changes in recently deposited till from south-east Iceland. *Geogr. Ann.,* **56A**(3–4), 121–134.

Boulton, G.S. and R.C.A. Hindmarsh. 1987. Sediment deformation beneath glaciers: rheology and geological consequences. *J. Geophys. Res.,* **92**(B9), 9059–9082.

Boulton, G.S., D.L. Dent and E.M. Morris. 1974. Subglacial shearing and crushing, and the role of water pressures in tills from south-east Iceland. *Geogr. Ann.,* **56A**(3–4), 135–145.

Boulton, G.S., K.E. Dobbie and S. Zatsepin. 2001. Sediment deformation beneath glaciers and its coupling to the subglacial hydraulic system. *Quat. Int.,* **86**(1), 3–28.

Clarke, G.K.C. 1987. Subglacial till: a physical framework for its properties and processes. *J. Geophys. Res.,* **92**(B9), 9023–9036.

https://doi.org/10.3189/172756405781812961 Published online by Cambridge University Press

Dowdeswell, J.A. and M.J. Sharp. 1986. Characterization of pebble fabrics in modern terrestrial glacigenic sediments. *Sedimentology,* **33**(5), 699–710.

Dreimanis, A. 1988. Tills: their genetic terminology and classification. *In* Goldthwait, R.P. and C.L. Matsch, *eds. Genetic classification of glacigenic deposits*. Rotterdam, A.A. Balkema, 17–83.

Engelhardt, H. and B. Kamb. 1998. Basal sliding of Ice Stream B, West Antarctica. *J. Glaciol.,* **44**(147), 223–230.

Evans, D.J.A. 2000. A gravel outwash/deformation till continuum, Skalafellsjokull, Iceland. *Geogr. Ann.,* **82A**(4), 499–512.

Evans, D.J.A. 2003. *Glacial landsystems. Second edition.* London, Edward Arnold.

Evans, D.J.A., D.S. Lemmen and B.R. Rea. 1999. Glacial landsystems of the southwest Laurentide ice sheet: modern Icelandic analogues. *J. Quat. Sci.,* **14**(7), 673–691.

Eyles, N., C.H. Eyles and A. Miall. 1983. Lithofacies types and vertical profile models: an alternative approach to the description and environmental interpretation of glacial diamict and diamictite sequences. *Sedimentology,* **30**(3), 393–410.

Fischer, U.H. and G.K.C. Clarke. 1997. Stick–slip sliding behaviour at the base of a glacier. *Ann. Glaciol.,* **24**, 390–396.

Fischer, U.H. and G.K.C. Clarke. 2001. Review of subglacial hydromechanical coupling: Trapridge Glacier, Yukon Territory, Canada. *Quat. Int.,* **86**, 29–43.

Fischer, U.H., G.K.C. Clarke and H. Blatter. 1999. Evidence for temporally varying ''sticky spots'' at the base of Trapridge Glacier, Yukon Territory, Canada. *J. Glaciol.,* **45**(150), 352–360.

Fuller, S. and T. Murray. 2000. Evidence against pervasive bed deformation during the surge of an Icelandic glacier. *In* Maltman, A.J., B. Hubbard and M.J. Hambrey, *eds. Deformation of glacial materials*. London, Geological Society of London, 203–216. (Geological Society Special Publication 176.)

Fuller, S. and T. Murray. 2002. Sedimentological investigations in the forefield of an Icelandic surge-type glacier: implications for the surge mechanism. *Quat. Sci. Rev.,* **21**(12–13), 1503–1520.

Hart, J.K. 1994. Till fabric associated with deformable beds. *Earth Surf. Process. Landforms,* **19**(1), 15–32.

Hart, J.K. and G.S. Boulton. 1991. The interrelation of glaciotectonic and glaciodepositional processes within the glacial environment. *Quat. Sci. Rev.,* **10**(4), 335–350.

Hart, J.K. and J. Rose. 2001. Approaches to the study of glacier bed deformation. *Quat. Int.,* **86**(1), 45–58.

Hicock, S.R. and E.A. Fuller. 1995. Lobal interactions, rheologic superimposition, and implications for a Pleistocene ice stream on the continental shelf of British Columbia. *Geomorphology,* **14**(2), 167–184.

Hooke, R.LeB. and N.R. Iverson. 1995. Grain-size distribution in deforming subglacial tills: role of grain fracture. *Geology* (Boulder), **23**(1), 57–60.

Hooyer, T.S. and N.R. Iverson. 2000. Clast-fabric development in a shearing granular material: implications for subglacial till and fault gouge. *Geol. Soc. Amer. Bull.,* **112**(5), 683–692.

Hubbard, B.P., M.J. Sharp, I.C. Willis, M.K. Nielsen and C.C. Smart. 1995. Borehole water-level variations and the structure of the subglacial hydrological system of Haut Glacier d'Arolla, Valais, Switzerland. *J. Glaciol.,* **41**(139), 572–583.

Humphrey, N., B. Kamb, M. Fahnestock and H. Engelhardt. 1993. Characteristics of the bed of the lower Columbia Glacier, Alaska. *J. Geophys. Res.,* **98**(B1), 837–846.

Iverson, N.R., P. Jansson and R.LeB. Hooke. 1994. In-situ measurement of the strength of deforming subglacial till. *J. Glaciol.,* **40**(136), 497–503.

Iverson, N.R., B. Hanson, R.LeB. Hooke and P. Jansson. 1995. Flow mechanism of glaciers on soft beds. *Science,* **267**(5194), 80–81.

Iverson, N.R. *and 6 others*. 2003. Effects of basal debris on glacier flow. *Science,* **301**(5629), 81–84.

Kamb, B. *and 7 others*. 1985. Glacier surge mechanism: 1982–1983 surge of Variegated Glacier, Alaska. *Science,* **227**(4686), 469–479.

Knight, P.G. 1994. Two-facies interpretation of the basal layer of the Greenland ice sheet contributes to a unified model of basal ice formation. *Geology* (Boulder), **22**(11), 971–974.

Knudsen, Ó. 1995. Concertina eskers, Brúarjökull, Iceland: an indicator of surge-type behaviour. *Quat. Sci. Rev.,* **14**(5), 487–493.

Knudsen, O. and P.M. Marren. 2002. Sedimentation in a volcanically dammed valley, Bruárjökull, northeast Iceland. *Quat. Sci. Rev.,* **21**(14–15), 1677–1692.

Lawson, D.E. 1979. Sedimentological analysis of the western terminus region of the Matanuska Glacier, Alaska. *CRREL Rep.* 79-9.

Mair, D., I. Willis, U.H. Fischer, B. Hubbard, P. Nienow and A. Hubbard. 2003. Hydrological controls on patterns of surface, internal and basal motion during three ''spring events'': Haut Glacier d'Arolla, Switzerland. *J. Glaciol.,* **49**(167), 555–567.

Menzies, J. 2000. Micromorphological analyses of microfabrics and microstructures indicative of deformation processes in glacial sediments. *In* Maltman, A.J., B. Hubbard and M.J. Hambrey, *eds. Deformation of glacial materials*. London, Geological Society of London, 245–257. (Geological Society Special Publication 176.)

Ó Cofaigh, C. and D.J.A. Evans. 2001. Deforming bed conditions associated with a major ice stream of the last British ice sheet. *Geology,* **29**(9), 795–798.

Paul, M.A. and N. Eyles. 1990. Constraints on the preservation of diamict facies (melt-out tills) at the margins of stagnant glaciers. *Quat. Sci. Rev.,* **9**(1), 51–69.

Piotrowski, J.A. and S. Tulaczyk. 1999. Subglacial conditions under the last ice sheets in northwest Germany: ice–bed separation and enhanced basal sliding? *Quat. Sci. Rev.,* **18**(6), 737–751.

Powers, M.C. 1953. A new roundness scale for sedimentary particles. *J. Sediment. Petrol.,* **23**(2), 117–119.

Raymond, C.F. 1987. How do glaciers surge? A review. *J. Geophys. Res.,* **92**(B9), 9121–9134.

Sharp, M. 1985. ''Crevasse-fill'' ridges – a landform type characteristic of surging glaciers? *Geogr. Ann.,* **67A**(3–4), 213–220.

Sigurðsson, O. 1998. Glacier variations in Iceland 1930–1995: from the database of the Iceland Glaciological Society. *Jökull,* **45**, 3–25.

Souchez, R., R. Lorrain, J.L. Tison and J. Jouzel. 1988. Co-isotopic signature of two mechanisms of basal-ice formation in Arctic outlet glaciers. *Ann. Glaciol.,* **10**, 163–166.

Stone, D.B. and G.K.C. Clarke. 1996. In-situ measurements of basal water quality and pressure as an indicator of the character of subglacial drainage systems. *Hydrol. Process.,* **10**(4), 615–628.

Thórarinsson, S. 1964. Sudden advance of Vatnajökull outlet glaciers 1930–1964. *Jökull,* **14**, 76–89.

Thórarinsson, S. 1969. Glacier surges in Iceland with special reference to the surges of Brúarjökull. *Can. J. Earth Sci.,* **6**(4), 875–882.

Van der Meer, J.J.M. 1987. Micromorphology of glacial sediments as a tool in distinguishing genetic varieties of till. *In* Kujansuu, R. and M. Saarnisto, *eds. INQUA Till Symposium, Finland 1985*. Espoo, Geological Society of Finland, 77–89. (Special Paper 3.)

Van der Meer, J.J.M. 1993. Microscopic evidence of subglacial deformation. *Quat. Sci. Rev.,* **12**(7), 553–587.

Van der Meer, J.J.M. 1997. Particle and aggregate mobility in till: microscopic evidence of subglacial processes. *Quat. Sci. Rev.,* **16**(8), 827–831.

Van der Meer, J.J.M., J. Menzies and J. Rose. 2003. Subglacial till: the deforming glacier bed. *Quat. Sci. Rev.,* **22**, 1659–1685.

https://doi.org/10.3189/172756405781812961 Published online by Cambridge University Press